

Nondestructive picosecond-ultrasonic characterization of Mo/Si extreme ultraviolet multilayer reflection coatings

Nen-Wen Pu^{a)} and Jeffrey Bokor

Department of Electrical Engineering and Computer Science, University of California, Berkeley, California 94720-1772

Seongtae Jeong

Center for X-ray Optics, Lawrence Berkeley National Laboratory, Berkeley, California 94720

Ri-An Zhao

Department of Material Science and Mineral Engineering, University of California, Berkeley, California 94720

(Received 2 June 1999; accepted 18 August 1999)

We have used noncontact, nondestructive picosecond-ultrasonic techniques to characterize Mo/Si multilayer reflection coatings for extreme ultraviolet (EUV) lithography. Using our alternating-pump technique, we successfully excited and detected the two lowest frequency localized acoustic-phonon surface modes. By measuring their vibration frequencies simultaneously, we can extract the two key parameters for EUV reflector performance: d (bilayer thickness) and Γ (thickness ratio of Mo layer to the bilayer) of the Mo/Si multilayers. To demonstrate the utility of this technique, we measured the surface-mode frequencies and extracted the values of d and Γ for six mirrors. Good agreement with the results of at-wavelength EUV reflectometry was found. Damage to coatings caused by the pump and probe laser beams was also studied, and found to be negligible given our data-acquisition time. © 1999 American Vacuum Society. [S0734-211X(99)10806-0]

I. INTRODUCTION

Extreme ultraviolet (EUV) lithography is made possible by the development of normal-incidence reflection coatings with relatively high reflectivity at wavelengths in the 10–15 nm range. Mo/Si multilayer coatings with reflectance of 67.5% at 13.4 nm and Mo/Be multilayers with reflectance of 70.2% at 11.4 nm are now routinely achieved.¹ Since these coatings have fairly narrow bandpass, and typically seven to eight optics are used for a prototype projection lithography system,² the wavelength of the peak reflectance must be all aligned to within 0.05 nm to preserve at least 90% of the optimum throughput.¹ For example, this requirement sets the run-to-run deposition reproducibility of Mo/Si bilayer thickness to within 0.025 nm (0.36%). In addition, to minimize the phase errors that affect the imaging performance, the deviation from the designed coating thickness profile across an optic must be less than 0.4%.³

In order to meet these stringent requirements, a good characterization technique is necessary to measure the physical period, d and the Γ ratio (thickness ratio of Mo layer to the bilayer), and to evaluate the uniformity and repeatability of the deposition process. Grazing incidence x-ray diffraction offers high accuracy in measuring d . However, the small grazing angle requirement, and the relatively large x-ray spot size (typically ~ 3 mm) greatly limit its usefulness and preclude its application in measuring curved optics and in evaluating coating uniformity. Another frequently used diagnostic tool, at-wavelength reflectance measurement, has the advantages of small spot size, near-normal incidence, and good

accuracy for d measurement. However, the high cost and limited access to EUV sources make this tool unavailable to many researchers. In addition, neither of these two techniques can separately measure Γ accurately.

Picosecond ultrasonics has proven to be a useful technique for the study and characterization of thin films, multilayers and other nanostructures.^{4–10} It is an optical, pump-and-probe transient reflectivity technique in which the acoustic waves are impulsively excited by optical absorption of an ultrashort, visible wavelength “pump” laser pulse and detected as a reflectivity change of a time-delayed visible “probe” laser beam. In a periodic multilayer structure, resonant acoustic vibrations may be thought of as “superlattice phonons.” A superlattice phonon dispersion curve for a Mo/Si multilayer with $d = 6.9$ nm and $\Gamma = 0.4$ is shown in Fig. 1. The opening of gaps (stop bands) and folding of the acoustic-phonon branch are due to the periodic boundary condition imposed by the multilayer structure. Sharp resonant modes existing within the frequency band gaps (one mode per gap, as indicated with arrows in Fig. 1) have been observed in many superlattices and multilayers. These modes are nonpropagating, persistent, and localized near the free surface of a multilayer stack. Hence, the name “localized surface modes.” For a semi-infinite Mo/Si multilayer structure, the vibration frequencies ν_n are given by¹⁰

$$\tan\left(\frac{2\pi\nu_n d(1-\Gamma)}{c_{\text{Si}}}\right) + \frac{\rho_{\text{Mo}}c_{\text{Mo}}}{\rho_{\text{Si}}c_{\text{Si}}}\tan\left(\frac{2\pi\nu_n d\Gamma}{c_{\text{Mo}}}\right) = 0, \quad (1)$$

where ρ_{Si} , ρ_{Mo} are the densities, and c_{Si} , c_{Mo} the sound velocities of the Si and Mo layers, respectively. n is the index for gaps or modes.

^{a)}Electronic mail: pun@eecs.berkeley.edu

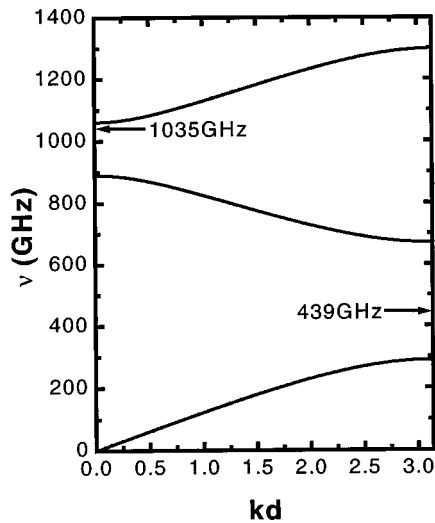


FIG. 1. Superlattice phonon dispersion curve for the acoustic branch in a Mo/Si multilayer with $d=6.8$ nm and $\Gamma=0.4$. ($\rho_{\text{Si}}=2.33$ g/cm³, $c_{\text{Si}}=6.9 \times 10^5$ cm/s; $\rho_{\text{Mo}}=10.22$ g/cm³, $c_{\text{Mo}}=6.2 \times 10^5$ cm/s.)

Recently, we reported successful excitation and detection of the lowest two surface modes in Mo/Si multilayers⁹ with coating periods varying from 32.6 down to 6.8 nm, which is the typical thickness for practical EUV lithography coatings. We also demonstrated the utility of this technique for characterization purposes by mapping the thickness profile of a linearly graded Mo/Si multilayer sample with 2% d variation.¹⁰ In Ref. 10, we also studied theoretically and experimentally the functional dependences of the frequencies on d and Γ . It was concluded that their effects are separable, and we can extract d and Γ simultaneously if any two surface-mode frequencies are known. In this article, we report experimental results on the simultaneous extraction of d and Γ using the picosecond ultrasonics technique, and compare our results with EUV reflectometry results.

II. EXPERIMENTAL SETUP

The schematic diagram of our experimental setup is shown in Fig. 2. The light pulses were produced by a mode-locked Ti:sapphire laser operating at 800 nm, with a full width at half maximum (FWHM) pulse duration of 120 fs and a repetition rate of 100 MHz. The pulses were focused onto an area of the sample with spot sizes of approximately 10 and 6 μm for pump and probe beams, respectively. The pump pulses deposit optical energy in the multilayer and impulsively excite acoustic waves in the structure. The optical absorption occurs predominantly in Mo layers with an absorption length of ~ 20 nm. An initial stress field is set up in the mechanical structure by the heat, and the relaxation of this stress field then launches strain waves (viz. ultrasonic waves) in the multilayer. A slight change of the optical reflectivity is induced by these strain waves, and is then detected by a time-delayed probe pulse. An auto-balanced detector circuit, which compares and balances the two inputs with an adjustable feedback-loop time constant, is used to help suppress low frequency laser noise. The delay time be-

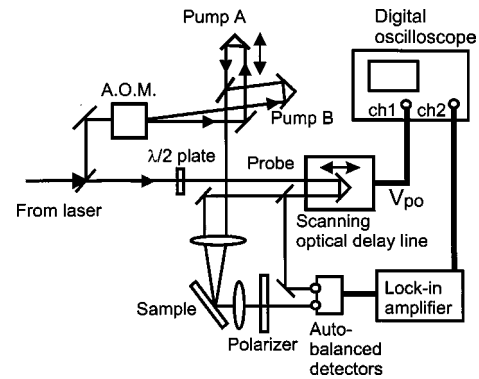


FIG. 2. Experimental setup (A.O.M.: acousto-optic modulator). Pumps A and B are, respectively, the zeroth- and the first-order diffracted beams from the A.O.M. The $\lambda/2$ plate is to rotate the polarization of the probe beam by 90° so that it can be separated from the scattered pump light by a polarizer. V_{po} : the position output of the scanning optical delay line.

tween pump and probe beams was varied by a scanning optical delay line driven by a 1.6 Hz sinusoidal wave. The controller of this optical delay scanner has a position output whose voltage (V_{po}) is proportional to the optical delay (τ). This position output and the probe beam signal were taken simultaneously and averaged 256 times by a digital oscilloscope in ~ 3 min. Thus, we can acquire and plot the traces of the reflected probe beam signal versus delay time τ .

The technical difficulty for probing the surface modes is that the vibrational response of interest is typically one to two orders of magnitude weaker than an interfering nonvibrational response of the materials, which itself is not large ($\Delta R_{\text{nonvib}}/R$ is usually on the order of 10^{-3} – 10^{-6}). Previously, we reported a successful picosecond ultrasonic measurement on Mo/Si multilayers using a novel ‘‘alternating-pump technique,’’⁹ which was demonstrated to enhance S/N by up to 20 dB. As shown in Fig. 2, two pump beams: A and B (instead of the single one in conventional pump-probe scheme), were used to excite the sample. Pump beams A and B are, respectively, the zeroth- and the first-order diffracted beams from an acousto-optic modulator (diffraction efficiency $\sim 90\%$). Thus, these two beams come alternately onto the sample at a 100 kHz modulation frequency, and the lock-in amplifier detects the difference of the responses excited by them. An extra advantage of our alternating-pump technique is that we can selectively reveal the weaker low-frequency mode (first gap) by canceling the high-frequency mode (second gap), and thus attain a higher measurement accuracy of ν_1 . (See Ref. 9 for more details about this technique.) The reason why the second-gap mode is stronger than the first-gap mode might be that, due to the spatial form of the initial stress or the ‘‘sensitivity function’’^{4,8} $f(z)$ (the contribution to ΔR due to the strain at a depth z), the latter is not appreciably excited and/or detected.^{5,6}

III. SIMULTANEOUS EXTRACTION OF d AND Γ

Evidently, in order to simultaneously extract the two parameters d and Γ , we need the data of at least two surface modes. It is apparent from Eq. (1) that, for each mode n , ν_n is

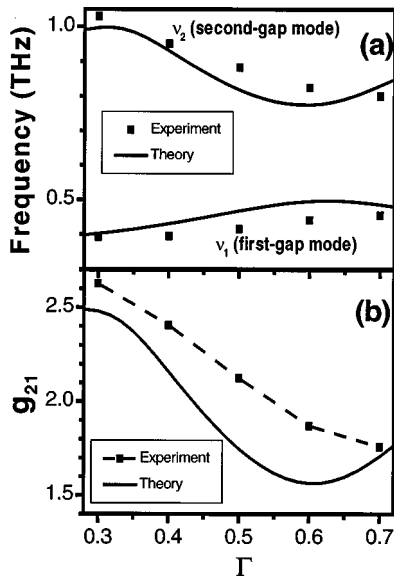


FIG. 3. (a) Vibration frequencies of the two surface modes vs Γ ($d = 6.9$ nm). (b) g_{21} (the ratio ν_2/ν_1) as a function of Γ . The solid lines are the theoretical predictions, and the filled squares are the measured values.

inversely proportional to d . In Ref. 10, we have shown that the ratio of the frequencies of any two modes g_{mn} (defined as ν_m/ν_n) is a function of Γ only, independent of d . Thus, Γ can be determined if it has one-to-one correspondence to g_{mn} . To achieve this, first, we need to establish a chart or a table of g as a function of Γ . As mentioned before, we observed the first and second surface modes in all of our Mo/Si multilayer samples. The theoretical and measured values of ν_1 , ν_2 , and g_{21} are plotted in Figs. 3(a) and 3(b). These samples have $d = 6.9$ nm, and their Γ values were determined by the product of deposition times and calibrated deposition rates for both materials, and do not include contraction due to silicide formation.¹¹ Due to the uncertainty of material parameters, and the formation of silicide interlayers, there is a slight mismatch between the theory and the real data, but they basically show the same tendency. Despite this mismatch, for characterization purposes, we have used the empirical data measured from these five samples as our reference, and read out the Γ value by interpolation between points.

The measurement reproducibility of the peak frequencies depends on the linewidth of vibration modes, which varies with Γ and d . For $d = 6.9$ nm and $\Gamma = 0.4$, the standard deviation is found to be 0.15% and 0.39% for ν_1 and ν_2 , respectively. The combined error for g_{21} is $\pm 0.54\%$, which corresponds to an absolute error of $\Delta\Gamma \sim \pm 0.005$ at $\Gamma = 0.4$, according to the experimental data in Fig. 3(b). Currently, there is no other nondestructive tool that offers this precision. Once Γ is obtained, d is found using

$$d/d_{\text{ref}} = \nu_{n_{\text{ref}}}(\Gamma)/\nu_n, \quad (2)$$

where $n = 1$ or 2 , d_{ref} is the bilayer thickness of the reference wafers in Fig. 3, and $\nu_{n_{\text{ref}}}(\Gamma)$ is the corresponding surface-mode frequency interpolated at the determined Γ value [us-

ing the reference data points in Fig. 3(a)]. Five data points are too sparse indeed for an accurate estimate using interpolation, but it suffices for our preliminary trial for evaluation purposes.

To evaluate the utility of our technique, the coating team at Lawrence Livermore National Laboratory provided seven sample coatings deposited on silicon wafers for us to test, and later compared our results with the at-wavelength EUV reflectance measurements done at the Advanced Light Source (ALS) synchrotron radiation facility at Lawrence Berkeley National Laboratory. We performed picosecond-ultrasonic measurement on five points around the center of each wafer [see the inset in Fig. 4(a) for the geometry]. One of the wafers was found defective because no vibration signals were detected, which was confirmed by the EUV reflectance measurement. Figures 4(a) and 4(b) show the measured vibration frequencies ν_1 and ν_2 , respectively, for the other six wafers. The values of Γ and d extracted from ν_1 and ν_2 are shown in Figs. 4(c) and 4(d), respectively (solid squares). d was calculated and plotted relative to d_{ref} , the period of the reference samples of Fig. 3. For comparison, the peak wavelength of EUV reflectance (λ_{EUV}) for each wafer is also shown in Fig. 4(d) (open triangles), plotted relative to $\lambda_{\text{EUV}_{\text{ref}}}$, the peak EUV reflectance wavelength for the reference samples ($d_{\text{ref}} = 6.90$ nm and $\lambda_{\text{EUV}_{\text{ref}}} = 13.44$ nm). All of these wavelengths are measured near the center of each wafer. From Bragg's law, the period d is proportional to λ_{EUV} . Therefore, d/d_{ref} and $\lambda_{\text{EUV}}/\lambda_{\text{EUV}_{\text{ref}}}$ can be directly compared.

We observed a systematic offset of the two data sets in Fig. 4(d). A 0.6% relative shift of either set of data (the open circles, for example) will make them agree to within the measurement error bar. The most likely cause for this offset is calibration drift of our measurement system, and in particular, the optical delay scanner, because of its mechanical nature. To verify this, we recalibrated it and found that indeed, the proportionality constant between the position output voltage V_{po} and the delay time τ had already shifted by $\sim 1\%$ in the last year. This can easily explain the offset because the reference wafers were measured five months before the test wafers, and the measured frequencies need to be corrected by the amount of miscalibration. Thus, the measurement accuracy of our current experimental setup is probably limited by this device. Frequent calibration can solve this problem, but a better solution is to use a more reliable way of real-time position detection such as optical interferometry, which is a mature technology and offers sub-micron precision. Besides this, there is still much room for us to improve our measurement precision and accuracy. For example, a better signal filtering/processing algorithm might improve the accuracy of the extraction of ν_1 and ν_2 . Also, more reference data points around $\Gamma = 0.4$ can give a more accurate interpolation estimate of Γ . However, our preliminary results already demonstrate the viability of sample characterization using this new technique.

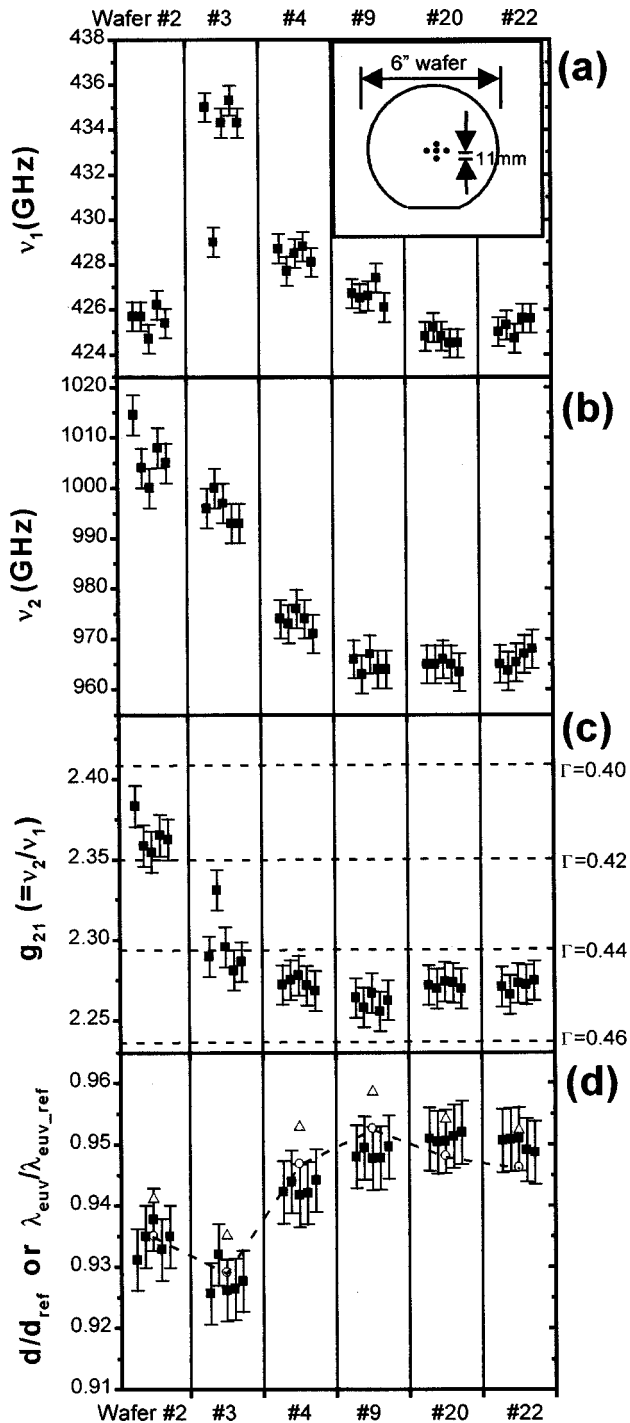


FIG. 4. (a) and (b) measured frequencies ν_1 and ν_2 for test wafers. The inset in (a) shows the measurement geometry: ν_1 and ν_2 are measured on five points near the center of each wafers. (c) g_{21} (or Γ) for test wafers. (d) Comparison of d/d_{ref} (solid squares) extracted from ν_1 and ν_2 , and $\lambda_{EUV}/\lambda_{EUV_ref}$ (triangles) measured by EUV reflectometry. A 0.6% relative shift of the two sets of data (open circles) makes them agree to within the error bar.

IV. LASER DAMAGE TO THE MULTILAYERS

We also observed damage to the multilayer coating due to laser heating. A 1.9% drop of vibration frequency ν_1 was detected under 1 h of continuous laser illumination with an

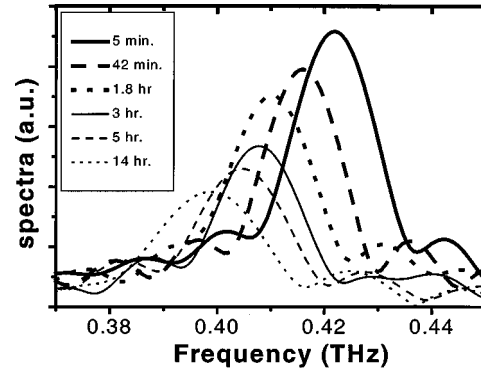


FIG. 5. Vibration spectra of the first-gap mode after various amount of laser illumination time.

intensity of 32 kW/cm^2 . Figure 5 shows the vibration spectra of the first-gap mode after varying amount of illumination time. The peak frequency ν_1 decreases by 5.4% and reaches an asymptote after $\sim 14 \text{ h}$. The vibration strength of this mode also decays monotonically with time. In contrast to the decrease in ν_1 , the peak frequency of the second-gap mode remains almost unchanged ($\sim 0.8\%$ increase after 7 h).

We speculate that this laser damage effect might be due to (1) the growth of silicide interdiffusion layers, or (2) the growth of a surface oxide layer. Chen *et al.* have considered the oxidation effect of the topmost layer on the surface-mode frequencies.⁵ The surface-mode frequencies can vary as much as 10% during surface layer oxidation. The exact numerical analysis of the frequency shift due to silicide formation cannot be carried out by our naive two-layer theory and needs to consider a four-layer structure in the theory. The growth of silicide interlayers can smear the abrupt acoustic-impedance mismatch between Si and Mo layers and thus will reduce the amplitude of the surface modes. Further experiment and analysis are needed to elucidate the precise origin for this frequency shift. The effect of laser damage on the peak wavelength and reflectance of EUV radiation is yet to be investigated. We also found that the laser damage effect is localized within the spot size of the pump laser beam, as evidenced by a negligible frequency shift at a distance of $10 \mu\text{m}$ from the center of the spot.

Although this damage effect is a potential disadvantage of our technique, we believe that it is not of significant concern. The data-acquisition time required to measure at a single point on the multilayer is only $\sim 3 \text{ min}$, which would lead to a shift of only $\sim 0.1\%$. Also, the damage is localized within a very small region of only $10 \mu\text{m}$ in diameter. In applications where even this could not be tolerated, measurements could be made in areas of a coating outside the critical area.

V. CONCLUSIONS

In conclusion, we have demonstrated the utility of our picosecond-ultrasonic technique for characterizing Mo/Si EUV multilayer coatings. The first and the second acoustic-phonon surface modes were observed in Mo/Si multilayers using the alternating-pump technique. By measuring ν_1 and

ν_2 simultaneously, we successfully extracted the two important parameters d and Γ for Mo/Si multilayers. Apart from a systematic offset, probably due to calibration drift, our results are in agreement with EUV reflectance measurements. The damage to multilayers caused by laser illumination were also studied. This technique can also be applied to other similar multilayers and superlattices.

ACKNOWLEDGMENTS

The authors thank Patrick Kearny at Lawrence Livermore National Laboratory for providing the reference and test samples. They also thank Marco Wedowsky for providing the results of EUV reflectometry measurements. This work is supported by the Semiconductor Research Corporation under Contract No. 96-LC-460, DARPA Advanced Lithography Program under Grant No. MDA972-97-0010, and AFOSR under Grant No. F49620-97-1-0220.

- ¹C. Montcalm, S. Bajt, P. B. Mirkarimi, E. Spiller, F. J. Weber, and J. A. Folta, Proc. SPIE **3331**, 42 (1998).
- ²D. W. Sweeney, R. M. Hudyma, H. N. Chapman, and D. R. Shafer, Proc. SPIE **3331**, 2 (1998).
- ³E. Spiller, F. J. Weber, C. Montcalm, S. L. Baker, E. M. Gullikson, and J. H. Underwood, Proc. SPIE **3331**, 62 (1998).
- ⁴H. T. Grahm, H. J. Maris, and J. Tauc, Phys. Rev. B **38**, 6066 (1988).
- ⁵W. Chen, Y. Lu, H. J. Maris, and G. Xiao, Phys. Rev. B **50**, 14506 (1994).
- ⁶B. Perrin, B. Bonello, J. C. Jeannet, and E. Romatet, Physica B **219&220**, 681 (1996).
- ⁷B. Bonello, B. Perrin, E. Romatet, and J. C. Jeannet, Ultrasonics **35**, 223 (1997).
- ⁸H. T. Grahm, H. J. Maris, and J. Tauc, IEEE J. Quantum Electron. **25**, 2562 (1989).
- ⁹N. W. Pu, S. Jeong, R-A. Zhao, and J. Bokor, Appl. Phys. Lett. **74**, 320 (1999).
- ¹⁰N. W. Pu, S. Jeong, R-A. Zhao, and J. Bokor, Proc. SPIE **3676**, 627 (1999).
- ¹¹R. S. Rosen, D. G. Stearns, M. A. Viliardos, M. E. Kassner, S. P. Vernon, and Y. Cheng, Appl. Opt. **32**, 6975 (1993).